

# Robust satellite techniques for monitoring volcanic eruptions

Nicola Pergola<sup>(1)</sup>, Carla Pietrapertosa<sup>(1)</sup>, Teodosio Lacava<sup>(2)</sup> and Valerio Tramutoli<sup>(2)</sup>

<sup>(1)</sup> Istituto di Metodologie Avanzate di Analisi Ambientale, CNR, Tito Scalo (PZ), Italy

<sup>(2)</sup> Università della Basilicata, DIFA, Potenza, Italy

## Abstract

Through this paper the robust approach to monitoring volcanic aerosols by satellite is applied to an extended set of events affecting Stromboli and Etna volcanoes to assess its performance in automated detection of eruptive clouds and in monitoring pre-eruptive emission activities. Using only NOAA/AVHRR data at hand (without any specific atmospheric model or ancillary ground-based measurements) the proposed method automatically discriminates meteorological from eruptive volcanic clouds and, in several cases, identified pre-eruptive anomalies in the emission rates not identified by traditional methods. The main merit of this approach is its effectiveness in recognising field anomalies also in the presence of a highly variable surface background as well as its intrinsic exportability not only on different geographic areas but also on different satellite instrumental packages. In particular, the possibility to extend the proposed method to the incoming new MSG/SEVIRI satellite package (which is going to fly next year) with its improved spectral (specific bands for SO<sub>2</sub>) and temporal (up to 15 min) resolutions has been evaluated representing the natural continuation of this work.

**Key words** *satellite remote sensing – AVHRR – robust techniques – volcanic aerosols detection*

## 1. Introduction

Remote sensing of volcanic activities from the U.S. National Oceanic and Atmospheric Administration (NOAA) satellites has been performed up to now on a global scale mainly in order to investigate their impact on weather and climate-related phenomena. Quantitative measurements of aerosol parameters like optical thickness, complex refraction index and size distribution were usually carried out matching satellite sensor data with a library of synthetic radiances computed for several realistic atmospheres with variable aerosol burden and properties

(Kaufman and Sendra, 1988; Masuda *et al.*, 1988; Rao *et al.*, 1988, 1989; Wen and Rose, 1994).

Satellite-based measurements at shorter space-time scales have been especially devoted to monitoring events like dust or volcanic clouds which, even if not always considerable for their climatic effects, could represent a potential danger for aircraft (Hanstrum and Watson, 1983; Casadevall, 1994).

In these cases, the most important application of satellite-based observations (regarding not only geo-stationary platforms) could be an early warning of the event in progress in order to mitigate hazards and damage (Prata, 1989; D'Amours, 1994; Rose and Schneider, 1996).

Generally speaking, all satellite-based techniques, devoted to giving a quantitative description of atmospheric aerosol properties, require ancillary information (usually coming from ground-based observations performed in coincidence with satellite passes or organised and updated in some climatological database) or rest

*Mailing address:* Dr. Nicola Pergola, Istituto di Metodologie Avanzate di Analisi Ambientale, CNR, C.da S. Loja, 85050 Tito Scalo (PZ), Italy; e-mail: pergola@imaaa.pz.cnr.it

on a number of hypotheses, which substantially reduce their applicability at the local scale and their reliability at the global scale. In fact, space-time variability of atmospheric aerosol burden and composition as well as Earth surface properties, mean that the requested assumptions are not always met locally. On the other hand, reliable coincident ancillary data, are only occasionally available at the requested space-time resolutions.

Satellite-based techniques, devoted to extreme events detection, find their main difficulties in discriminating volcanic aerosol layers from meteorological clouds. Both of them, in fact, typically reflect in the visible part of sun's spectrum and absorb Earth radiation in the thermal infrared so that refined techniques are required to discriminate between them.

Several methods have been suggested for this purpose based both on Advanced Very High Resolution Radiometer (AVHRR) visible and near infrared reflectances (Lyons and Husar, 1976; Rao *et al.*, 1989) and on thermal infrared radiances (Rao *et al.*, 1988; Wen and Rose, 1994). For example the technique proposed by Prata (1989) exploits the reverse absorption effect which is expected to lead, in thermal infrared channel 4 and channel 5, to negative values of the difference  $T_4 - T_5$  in the presence of  $H_2SO_4$  droplets in opposition to the positive values which are expected for water/ice clouds. Other authors noted that although both water/ice clouds and atmospheric aerosols layers increase the albedo in the visible and near infrared bands, that does not happen in the same way (Lyons and Husar, 1976). It has been found (Rao *et al.*, 1989) that for aerosols over oceans the effect is stronger in the visible AVHRR channel 1 than in the near infrared AVHRR channel 2, so that the ratio of albedos measured in channel 1 and channel 2 can be used to discriminate volcanic clouds from water/ice clouds. Rao *et al.* (1989) proposed a new technique that, in addition to cloud screening criteria based on the visible and near infrared reflectances, exploits the thermal infrared AVHRR channel 3, 4 and 5 in order to distinguish atmospheric aerosols from meteorological clouds.

Once water/ice clouds have been excluded, volcanic aerosols remain to be identified and

possibly described in terms of their physical and optical properties.

Both a quantitative description of aerosol properties and the simple detection of localised field-anomalies would benefit from more knowledge of local features (like surface temperature and reflectance and *normal* atmospheric aerosols burden) which is practically impossible to obtain at the required space-time resolution using only ground-based observations.

In this paper, following the *robust* approach proposed by Tramutoli (1998), a satellite-based method is presented, able to detect automatically and without any other ancillary information, anomalous atmospheric aerosol burden due to volcanic activities.

The global coverage, low-cost and high repetition rate offered by NOAA satellites together with the spatial resolution and spectral capabilities of their AVHRR sounders, have been considered to support the daily monitoring of the increased atmospheric aerosols burden related to potentially dangerous volcanic events. An approach to daytime detection over the sea will be presented here and the results discussed after its application to major and minor events related to Mt. Etna and Mt. Stromboli volcanoes' eruptive activity. One case is also presented of Etna's possible pre-eruptive activity, detected by means of such a method.

The proposed technique heavily relies on the present «Istituto di Metodologie Avanzate di Analisi Ambientale (IMAAA)» facilities for receiving, archiving and processing NOAA/AVHRR data. High speed data transfer and processing as well as extended archiving capability permitted an easy and automatic management of a long series of historical AVHRR data as well as a routine production and updating of reference fields.

## 2. Data and instruments

The NOAA Polar Orbiting Weather Satellites (POES) are sun-synchronous, near-polar orbiting platforms, designed to operate at an altitude of about 800 km with an orbital period of about 102 min which produces 14.1 orbits per day. Operating in pairs, they assure a global



coverage of the Earth with a repetition rate not longer than 6 h. The Advanced Very High Resolution Radiometer (AVHRR) is a five-channel scanning radiometer flying aboard NOAA/POES. It is able to measure the total solar reflected radiance at the top of the atmosphere (in the visible and near infrared bands) as well as the outgoing long-wave radiance, emitted by the Earth-atmosphere system, in the infra-red part of the electromagnetic spectrum. Table I summarises the five AVHRR bands. The spatial resolution at ground level is 1.1 km in nadir-view configuration.

NOAA/AVHRR data were collected and pre-processed in order to build a complete and dense data set. AVHRR radiances in channel 1 (visible) and in channel 2 (near-infrared) were calibrated in reflectances whereas thermal infrared channels (channel 3, 4 and 5) were converted into Brightness Temperatures (BT) following the standard procedure described in Lauritson *et al.* (1979) and Rao and Chen (1996).

A special attention was given to the image geo-referencing and therefore a precise image navigation were carried out following the technique proposed by Rosborough *et al.* (1994). Ground Control Points (GCPs) together with an iterative best-correlation method, developed at the IMAAA (Pergola and Tramutoli, 2000), were used to correct the satellite altitude angles, roll, pitch and yaw, obtaining a final navigation accuracy estimated to be within one AVHRR pixel.

In order to deal with a reference data set as homogeneous as possible, all analysed satellite scenes were chosen on the basis of some *similarity* characteristics: hour of pass (only passes between 11.00 and 15.00 GMT have been selected), annual period (monthly series have been

preferred), etc. All analysed passes, from 1980 until 1998, were collected at the IMAAA High Resolution Picture Transmission (HRPT) Receiving Station or obtained from the Satellite Station of the University of Dundee.

### 3. Volcanic clouds detection: the algorithm

AVHRR data were used to automatically detect tropospheric aerosol layers, due to volcanic activity, over the study area shown in fig. 1. The whole proposed method is described in detail in the following.

#### 3.1. Discrimination between volcanic aerosol and meteorological clouds

The main problem in volcanic aerosols detection is their discrimination from meteorological clouds. Several techniques have been proposed to date to do that and in this work some of them were tested on different minor and major Stromboli and Etna volcanic events. For instance, the method proposed by Prata (1989), which should lead to negative values of the difference  $T_4 - T_5$  between the brightness temperatures measured in AVHRR channel 4 and channel 5 in the presence of volcanic clouds, was tested. Results suggest that such a method, although preferable because of its applicability both in night and day conditions, seems, however, to be not very effective in the case of very «fresh» volcanic clouds, which contain water droplets and/or ice particles and then are very difficult to distinguish from meteorological clouds in the IR data (Wen and Rose, 1994), as well as in the case of very weak gas or ash emissions.

Moreover the channel 1/channel 2 ratio test was also applied, in conjunction with a series of volcanic events to evaluate its capability in volcanic cloud recognition. It has been demonstrated, in fact, that values from 1.75 to 2 of this ratio over oceans are characteristic of aerosols layers, the water/ice clouds having, on the other hand, a ratio near to or less than 1. Such a screening test resulted more suitable for weak anomalies detection, remaining, however, obviously not applicable in night-time conditions. Figure 2

**Table I.** AVHRR spectral characteristics: frequency ranges indicate the band-width for every channel.

| Channel | Frequency (nm) |
|---------|----------------|
| 1       | 580- 680       |
| 2       | 725-1000       |
| 3       | 3550-3930      |
| 4       | 10300-11300    |
| 5       | 11400-12400    |

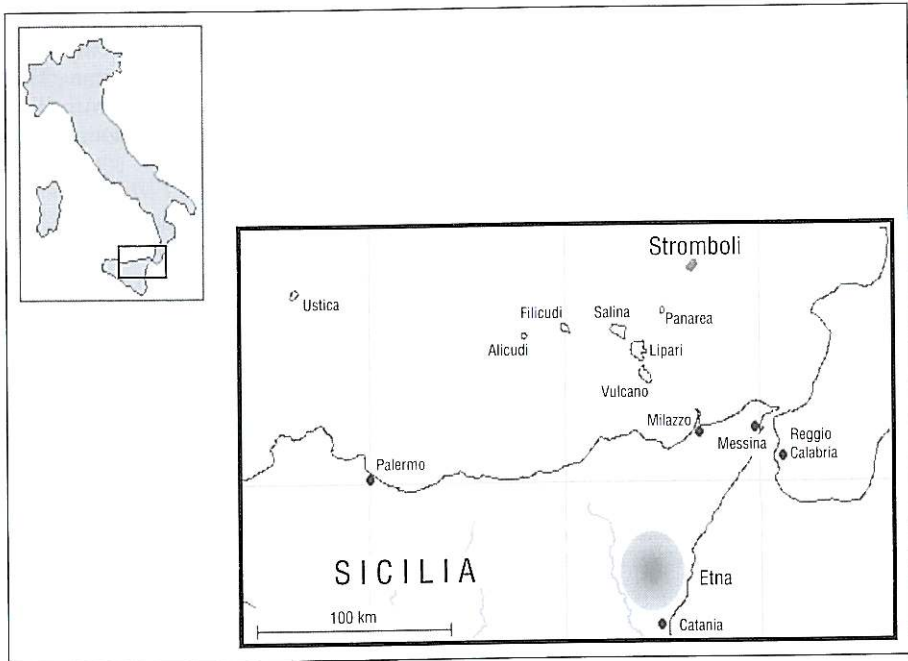


**Fig. 1.** The study area: Mt. Etna (summit elevation: 3350 m; location: 37.7°N, 15.0°E); Mt. Stromboli (summit elevation: 924 m; location: 38.789°N, 15.213°E).

shows the results obtained applying the ratio test on an AVHRR scene acquired just during an Etna eruption on 23 December 1995; on the left side AVHRR channel 1 reflectance field is reported where higher reflecting pixels, probably cloudy, are depicted in brighter grey tones; on the right side, test results are shown: pixels flagged as cloud-free are in black. It should be noted as such a test seems able to well discriminate between volcanic and meteorological clouds, automatically excluding the latter from further analysis. By applying such a test to all selected imagery, an automatic discrimination has performed and only pixels declared cloud-free were retained for the following steps.

### 3.2. Construction of the reference fields

In order to detect possible anomalies in the atmospheric aerosol burden the next step to be completed is to acquire information as complete

as possible (in a statistical sense) of the normal conditions of the area to be investigated. To do that we analysed, over the study area, an historical series of AVHRR images selected in unperturbed conditions (no volcanic clouds in the sensor's field of view) and with the above mentioned similarity characteristics. As affirmed before, aerosols and clouds, observed from space in the visible part of the electromagnetic spectrum, have the same behaviour: they show a high reflecting response and therefore produce an increase in the signal measured by the sensor carried by the satellite. Over low albedo surfaces, like oceans, an increase in the total reflected radiation measured by the sensor at the top of the atmosphere could be linearly correlated to an increase in atmospheric turbidity, the surface contribution being negligible (Masuda *et al.*, 1988).

Reflectance fields (in AVHRR channel 1) were derived for each satellite pass and a minimum Value Composite (mVC) filter was ap-

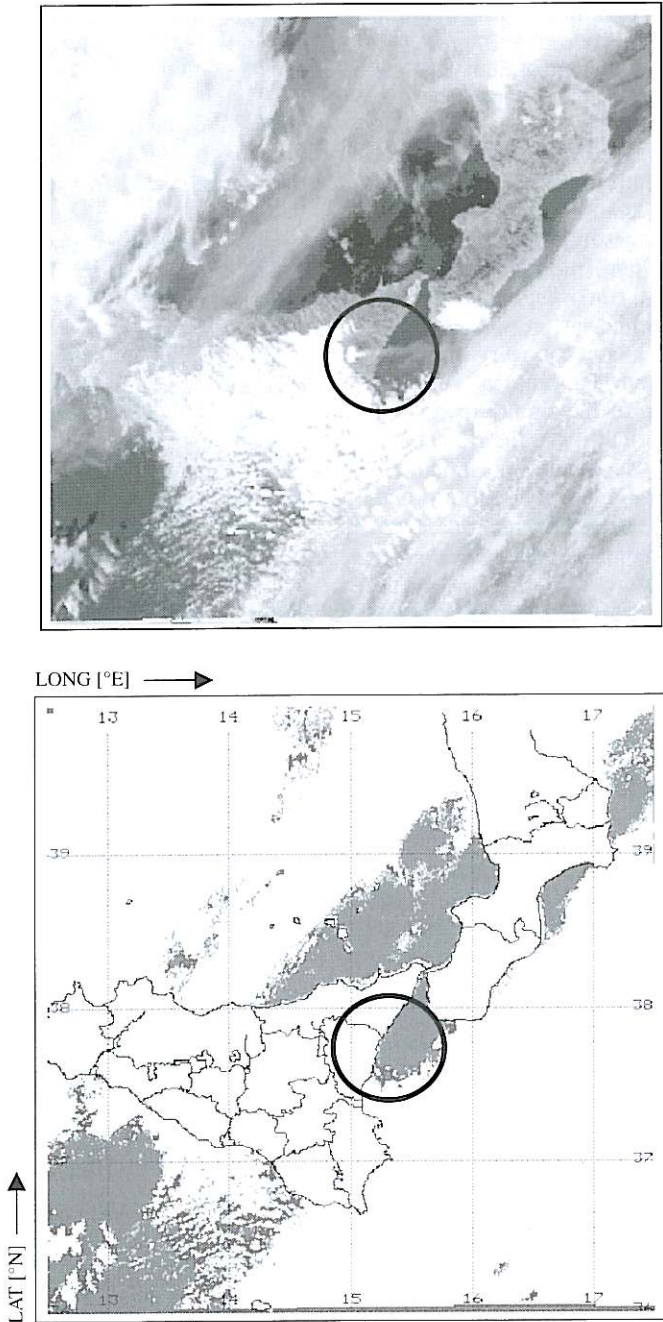


**Fig. 2.** Ch1/Ch2 ratio test results. Top: AVHRR channel 1 - the more reflective areas (clouds) are depicted in brighter grey tones. Bottom: ratio test results - the locations (over sea only) identified as cloud-free are coloured in grey.



plied to build a «background» monthly reference field,  $\rho_{\min}(x, y, m)$ . For every sea location  $(x, y)$  and for every month  $m$  of the year, the minimum value of reflectance  $\rho(x, y)$ , derived from all the co-located imagery, was retained so that  $\rho_{\min}(x, y, m)$  will represent, for construction, conditions of maximum atmospheric transparency. Besides the reflectance minimum field, on the same series of images, and considering only contributions from cloud-free pixels, the average reflectance  $\langle \rho(x, y, m) \rangle$  and the standard deviation  $\sigma(x, y, m)$  fields were computed, again for every location  $(x, y)$  and for every month  $m$ . The standard deviation takes into account the historical fluctuations of the signal, measuring locally the normal variability of the reflectance field, due to natural sources and not related to any volcanic activity. Obviously such a procedure will be more effective the larger and better the quality of the imagery collection.

The minimum reference field, derived as described above, allows us to eliminate automatically, all noisy contributions coming from residual thin clouds or from image-to-image differences related, for example, to the sun-satellite relative position. Nevertheless, possible spurious effects still remain, producing a decrease in the reflectance field not related to an increased atmospheric transparency. This is the case, for example, of cloud shadows or oil spills over the sea, whose effect could be a dramatic loss of the signal in the visible band of the satellite sensor also in presence of a turbid atmosphere (Böhm *et al.*, 1991; Legg, 1991; Stephens and Matson, 1993). In order to avoid such a problem, a further screening procedure was applied to the imagery. After reference fields were computed, for each measurement  $\rho(x, y)$  the following quantity has evaluated:

$$\Delta\rho(x,y) = |\rho(x, y) - \langle \rho(x, y, m) \rangle|.$$

For each location  $(x, y)$ , the measurement  $\rho(x, y)$  was flagged as anomalous, and excluded for further analysis, if  $\Delta\rho(x, y) > 3\sigma(x, y, m)$  (3-sigma clipping filter). After that a new computation of background reference fields was performed, using only the measurements surviving after the previous clipping filter applica-

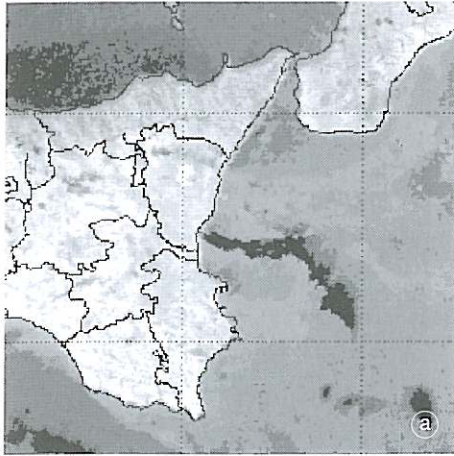
tion, obtaining the refined reference fields:  $\rho'_{\min}(x, y, m)$ ,  $\langle \rho'(x, y, m) \rangle$  and  $\sigma'(x, y, m)$ . The process could be iterate until no more data have to be excluded. Figure 3a-c is an example which shows how the above described clipping procedure was able to automatically detect a spurious minimum produced by a cloud shadow. In fig.3a the «rough» ( $\rho_{\min}(x, y, m)$ , before the clipping filter application) reference minimum field is shown whereas fig.3c shows the refined one ( $\rho'_{\min}(x, y, m)$ , after the filter). In this particular case, the considered month is December, so  $m = 12$ . As is clear, the major differences regard a long trail of low reflectance values (in dark grey tones) developing from the Sicily coast in a west-east direction. Looking at the fig. 3b, where a channel 1 reflectance field is shown for a single scene used for reference field generation (NOAA-14, orbit 10103 at 12.42.22 GMT, on 15 December 1996), it should be noted how such a trail was directly associated to the cloud shadow and then it was a spurious effect which the clipping procedure was able to automatically detect and eliminate.

### 3.3. Anomalous aerosol burden detection

A volcanic gas or ash emission into the atmosphere could be detected by satellite sensors as an anomaly, in the aerosol burden, compared to the *normal* atmospheric condition, *i.e.* the conditions in an unperturbed state. In order to do that, the Statistical Normalised Albedo Excess (Pergola *et al.*, 1998) defined by

$$\begin{aligned} \text{SNAE}(x, y, d) &= \\ &= [\rho(x, y, d) - \rho'_{\min}(x, y, m)] / \sigma'(x, y, m) \end{aligned}$$

where  $\rho(x, y, d)$  is the reflectance field for the AVHRR image to be processed (on current day  $d$ ), and  $\rho'_{\min}(x, y, m)$  and  $\sigma'(x, y, m)$  are the above defined background reference fields, computed for the month  $m$  (with  $d \in m$ ), was considered as an indicator of the local albedo excess weighted by the normal variability for each considered location  $(x, y)$ . SNAE  $(x, y, d)$  values greater than a pre-defined threshold could be considered as



anomalous and automatically detected by a simple computing procedure. It should be noted that such an indicator is valid locally but globally exportable and that it is very powerful in avoiding false alarms because it is weighted by the standard deviation  $\sigma'(x,y,m)$  which, taking into account the spectral historical behaviour of each location considered, leads to lower SNAE values for such locations with a normally high reflectance variability (like, for example, the areas in proximity of coasts, often contaminated by marine aerosol production).

#### 4. Results

In order to test our technique, the SNAE ( $x,y,d$ ) fields were computed for a series of AVHRR images acquired during some Etna and Stromboli volcanic events. Table II summarises the considered cases and the corresponding NOAA satellite passes. Some of these events, like the two on 24/09/86 and on 23/12/95 are well described in the literature as very violent ones, with heavy lava effusion and strong ash emissions. Others, like, for example, Etna's two on 12/01/91 and on 27/08/96 and the one of Stromboli on May 1996, could be related to an intense Strombolian activity in the periods considered. The last one, on 21/12/95 is not documented at all in the specialist literature and could be considered as a kind of *pre-eruptive* activity, since it occurred two days before the above mentioned Etna eruption of 23rd December 1995. In any case, such an event is, doubtless, a very weak one, characterised by low ash emission and/or gas injection into the atmosphere, which the proposed technique was able to automatically identify and detect. Figures from 4 to 6 show the results obtained, for the above mentioned events, coupled in chronological order; on the left side the AVHRR channel

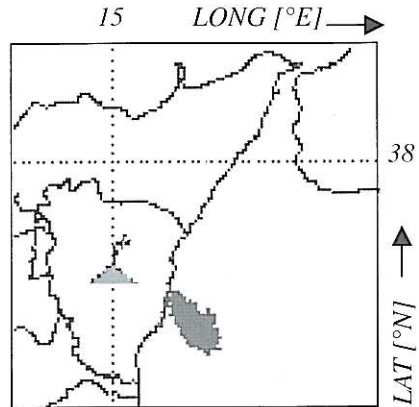
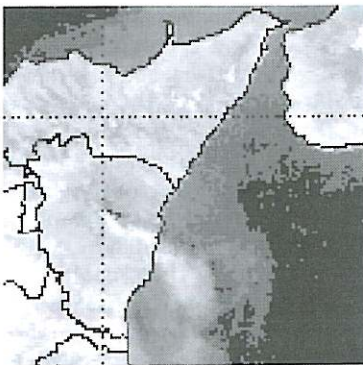
**Fig. 3a-c.** a) «Rough» minimum reference field  $\rho_{\min}(x,y,m)$  (see text); b) a cloud shadow image; c) refined minimum reference field  $\rho'_{\min}(x,y,m)$  after the  $3\sigma$  clipping filter application.



**Table II.** Details of the considered volcanic events together with the characteristics of corresponding analysed satellite passes.

| Index | Volcano   | Date              | Event description    | Satellite pass                  |
|-------|-----------|-------------------|----------------------|---------------------------------|
| I     | Etna      | 24 September 1986 | Eruptive activity    | NOAA-09 on 24/09/86 @ 13.30 GMT |
| II    | Etna      | 12 January 1991   | Strombolian activity | NOAA-11 on 12/01/91 @ 12.51 GMT |
| III   | Etna      | 21 December 1995  | Not documented       | NOAA-14 on 21/12/95 @ 12.33 GMT |
| IV    | Etna      | 23 December 1995  | Eruptive activity    | NOAA-14 on 23/12/95 @ 12.11 GMT |
| V     | Stromboli | 16 May 1996       | Strombolian activity | NOAA-14 on 16/05/96 @ 12.48 GMT |
| VI    | Etna      | 27 August 1996    | Strombolian activity | NOAA-14 on 27/08/96 @ 12.34 GMT |

Pass I



Pass II

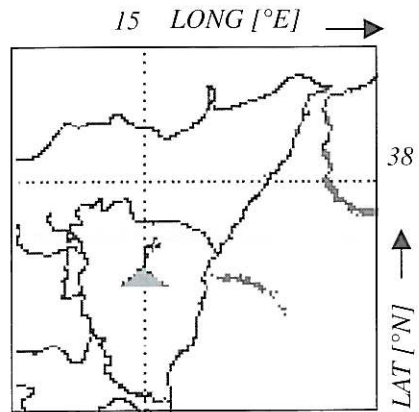
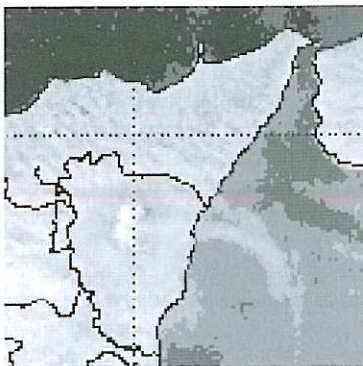


**Fig. 4.** Results shown for passes I (top) and II (bottom) in table II. Right side: SNAE fields; only pixels with a SNAE value greater than 3 are depicted in grey. Left side: corresponding AVHRR channel 1 reflectance fields.



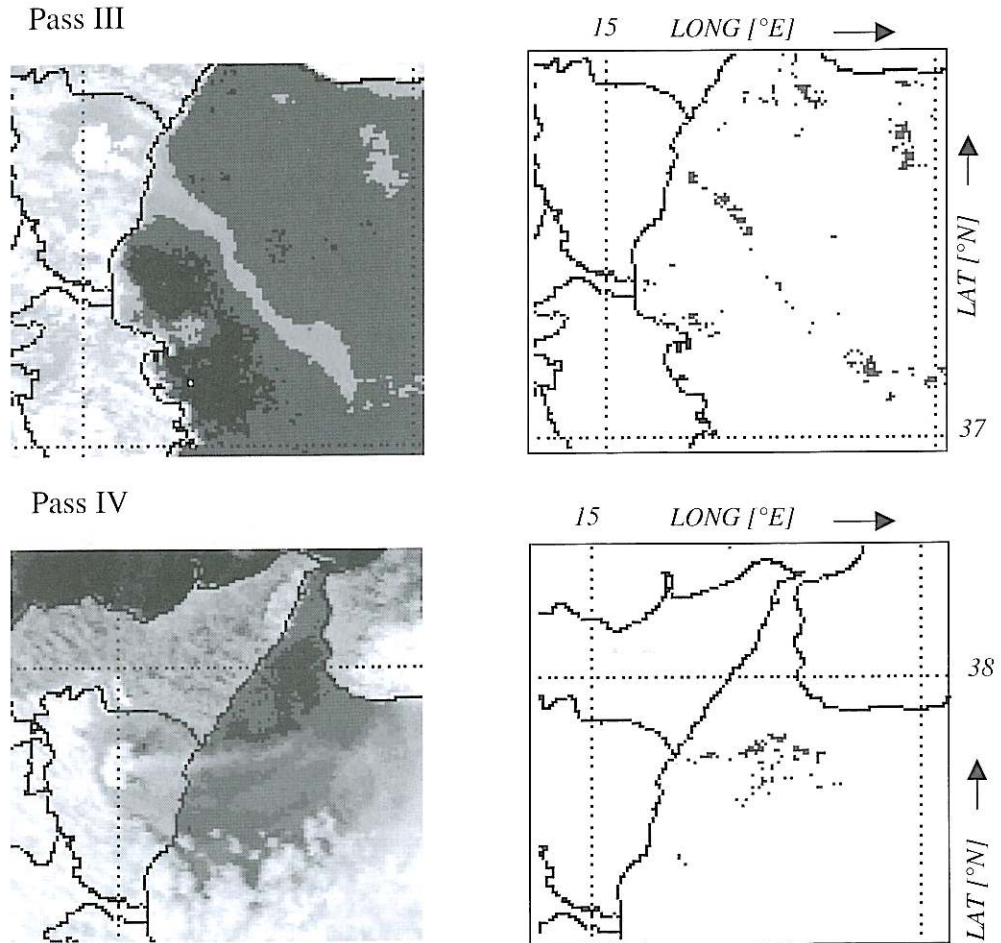


Fig. 5. As fig. 4 for passes III (top, with a threshold value of 2) and IV (bottom).

1 reflectance fields are reported whereas, on the right, only SNAE values greater than a threshold value (chosen equal to 2 for pass III and to 3 for all other passes) are depicted in black. Looking at these figures, it should be noted that the proposed technique, in all cases considered was automatically able to detect and recognise the volcanic clouds produced both by eruptive events and by simple weak emissions. It must be noted also how the proposed technique avoids the false alarms problem almost completely.

## 5. Final remarks

The technique proposed in this paper is strongly based on the analysis of homogeneous historical satellite datasets. It makes use of the advantages of a *local* and *seasonal* knowledge which, as obtained only from satellite data, can be easily exported to different geographical areas and seasons.

In a similar way, it could be immediately extended to the next generation of satellite sounders (*i.e.* SEVIRI which is going to fly

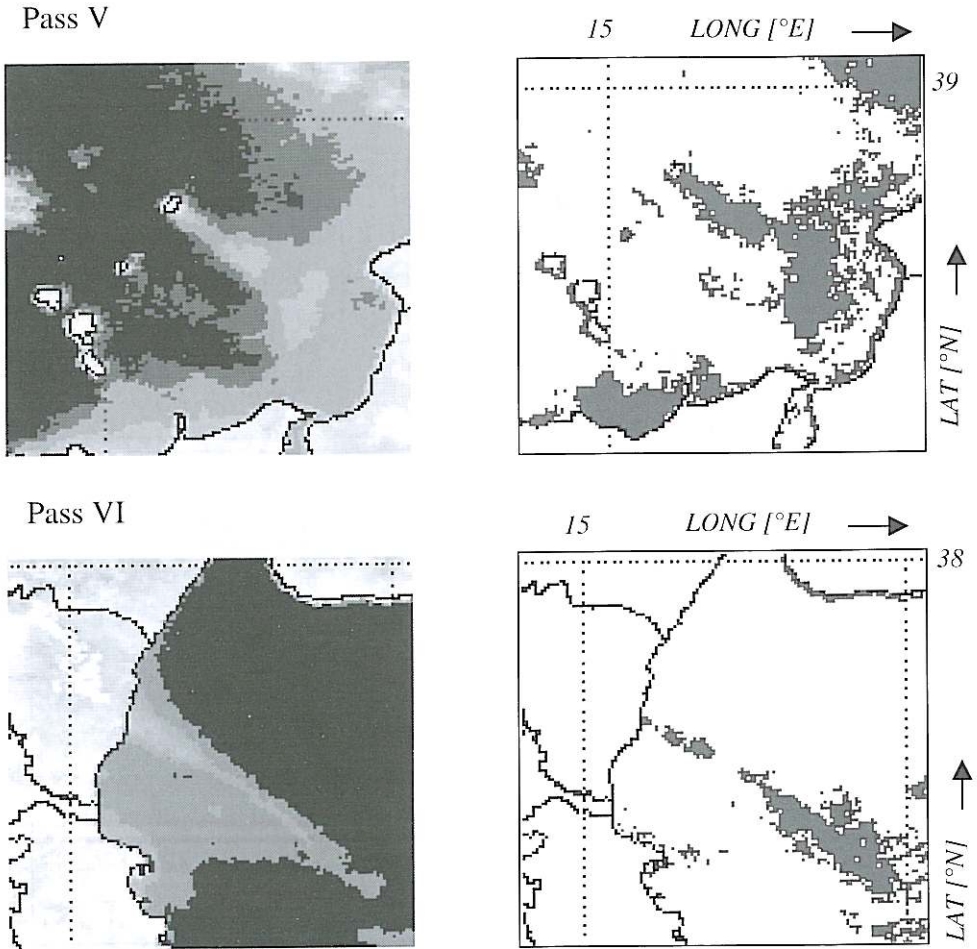


Fig. 6. As fig. 4 for passes V (top) and VI (bottom).

the next year on the Meteosat Second Generation platform) with improved capabilities in terms of repetition rate (one pass every 15 min!) and spectral resolution (a specific band for  $\text{SO}_2$ ).

Possible quantitative developments, together with improved performances also in different observational conditions (in night-time, over land) represent the natural continuation of such a work. Moreover, preliminary results concerning a possible pre-eruptive activity will be better investigated in the near future as well as its pos-

sible relationship with some other precursor effects (for instance the summital «hot spots» appearance) also detectable by satellite sensors.

#### Acknowledgements

This work was supported by the Italian Space Agency (ASI) and funded as «Progetto Pollino» jointly by European Community and Regione Basilicata in the context of POP-FESR 1994-1996.



## REFERENCES

- BÖHM, E., S. MARULLO and R. SANTOLERI (1991): AVHRR visible-IR detection of diurnal warming events in the Western Mediterranean Sea, *Int. J. Remote Sensing*, **12**, 695-701.
- CASADEVALL, T.J. (Editor) (1994): Volcanic ash and aviation safety: Proceedings of the first international symposium on volcanic ash and aviation, *U.S. Geol. Surv. Bull.* 2047, 450.
- D'AMOURS, R. (1994): Current and future capabilities in forecasting trajectories, transport, dispersion of volcanic ash clouds at the Canadian Meteorological Centre, volcanic ash and aviation safety, in *Proceedings of the First International Symposium on Volcanic Ash and Aviation*, edited by T.J. CASADEVALL, *U.S. Geol. Surv. Bull.* 2047, 325.
- HANSTRUM, B.N. and A.S. WATSON (1983): A case study of two eruptions of Mount Galunggung and an investigation of volcanic eruption cloud characteristics using remote sensing techniques, *Aus. Meteorol. Mag.*, **31**, 171-177.
- KAUFMANN, Y.J. and C. SENDRA (1988): Satellite mapping of aerosol loading over vegetated areas, in *Aerosols and Climate*, edited by P.V. HOBBS and M.P. MCCORMICK (Hampton, Virginia: A. Deepak Publishing), 51-67.
- LAURITSON, L., G.J. NELSON and F.W. PORTO (1979): Data extraction and calibration of TIROS-N/NOAA radiometers, *NOAA Technical Memorandum NESS 107*, U.S. Department of Commerce, Washington, D.C., U.S.A.
- LEGG, C.A. (1991): The Arabian Gulf oil slick, January and February 1991, *Int. J. Remote Sensing*, **12**, 1795-1796.
- LYONS, W.A. and R.B. HUSAR (1976): SMS/GOES visible images detect a synoptic-scale air pollution episode, *Mon. Weather Rev.*, **103**, 1623-1626.
- MASUDA, K., T. TAKASHIMA and C.R.N. RAO (1988): Remote sensing of atmospheric aerosols over the oceans using multispectral radiances measured with the Advanced Very High Resolution Radiometer onboard the NOAA meteorological satellites, in *Aerosols and Climate*, edited by P.V. HOBBS and M.P. MCCORMICK (Hampton, Virginia: A. Deepak Publishing), 38-49.
- PERGOLA, N. and V. TRAMUTOLI (2000): SANA: sub-pixel automatic navigation of AVHRR imagery, *Int. J. Remote Sensing Lett.*, **21** (12), 2519-2524.
- PERGOLA, N., C. PIETRAPERTOSA and V. TRAMUTOLI (1998): Satellite remote sensing of volcanic aerosols: a new, AVHRR-based, approach, in *Satellite Remote Sensing of Clouds and the Atmosphere III*, edited by E. RUSSEL, *Proc. SPIE*, **3495**, 188-197.
- PRATA, A.J. (1989): Observations of volcanic ash clouds in the 10-12  $\mu\text{m}$  window using AVHRR/2 data, *Int. J. Remote Sensing*, **10**, 751-761.
- RAO, C.R.N. and J. CHEN (1996): Post-launch calibration of the visible and near-infrared channels of the Advanced Very High Resolution Radiometer on the NOAA-14 spacecraft, *Int. J. Remote Sensing*, **17**, 2743-2747.
- RAO, C.R.N., L.L. STOWE, E.P. MCCLAIN and J. SAPPER (1988): Development and application of aerosol remote sensing with AVHRR data from the NOAA satellites, in *Aerosols and Climate*, edited by P.V. HOBBS and M.P. MCCORMICK (Hampton, Virginia: A. Deepak Publishing), 69-79.
- RAO, C.R.N., L.L. STOWE, E.P. MCCLAIN and J. SAPPER (1989): Remote sensing of aerosols over the oceans using AVHRR data. Theory, practice and applications, *Int. J. Remote Sensing*, **10**, 743-749.
- ROSBOROUGH, G.W., D.G. BALDWIN and W.J. EMERY (1994): Precise AVHRR image navigation, *IEEE Trans. Geosci. Remote Sensing*, **32**, 644-657.
- ROSE, W.I. and D.J. SCHNEIDER (1996): Satellite images offer aircraft protection from volcanic ash clouds, *Eos, Trans. Am. Geophys. Un.*, **77**, 529-530.
- STEPHENS, G. and M. MATSON (1993): Monitoring the Persian Gulf war with NOAA AVHRR data, *Int. J. Remote Sensing*, **14**, 1423-1429.
- TRAMUTOLI, V. (1998): Robust AVHRR Techniques (RAT) for Environmental Monitoring: theory and applications, in *Earth Surface Remote Sensing II*, edited by G. CECCHI and E. ZILIOI, *Proc. SPIE*, **3496**, 101-113.
- WEN, S. and W.I. ROSE (1994): Retrieval of sizes and total masses of particles in volcanic clouds using AVHRR bands 4 and 5, *J. Geophys. Res.*, **99**, 5421-5431.